

DexForce: Extracting Force-informed Actions from Kinesthetic Demonstrations for Dexterous Manipulation

Claire Chen¹, Zhongchun Yu¹, Hojung Choi¹, Mark Cutkosky¹, and Jeannette Bohg¹

Abstract—Imitation learning requires high-quality demonstrations consisting of sequences of state-action pairs. For contact-rich dexterous manipulation tasks that require fine-grained dexterity, the actions in these state-action pairs must produce the right forces. Current widely-used methods for collecting dexterous manipulation demonstrations are difficult to use for demonstrating contact-rich tasks due to unintuitive human-to-robot motion retargeting and the lack of direct haptic feedback. Motivated by this, we propose DexForce, a method for collecting demonstrations of contact-rich dexterous manipulation. DexForce leverages contact forces, measured during kinesthetic demonstrations, to compute force-informed actions for policy learning. We use DexForce to collect demonstrations for six tasks and show that policies trained on our force-informed actions achieve an average success rate of 76% across all tasks. In contrast, policies trained directly on actions that do not account for contact forces have near-zero success rates. We also conduct a study ablating the inclusion of force data in policy observations. We find that while using force data never hurts policy performance, it helps the most for tasks that require an advanced level of precision and coordination, like opening an AirPods case and unscrewing a nut. Videos can be found here: <https://clairelc.github.io/dexforce.github.io/>

I. INTRODUCTION

Successful dexterous manipulation hinges on applying the right forces, at the right times, in the right contact locations. This is especially important for fine-grained, contact-rich tasks, which demand a more nuanced application of forces than pick-and-place tasks. Consider opening an AirPods case (Fig. 1d) and flipping a box (Fig. 1e), which require applying precise forces at multiple contact points. Other tasks, such as grasping a thin camera battery (Fig. 1b) and unscrewing a nut (Fig. 1c) not only involve applying precise forces, but also require making and breaking contact with the object in a coordinated fashion. To succeed at contact-rich tasks like these, a robot must know how to apply the proper forces.

One way of teaching a robot how to apply the proper forces is through imitation learning [1]–[3]. Critically, successful imitation learning requires high-quality demonstrations consisting of sequences of state-action pairs. [4]. For contact-rich dexterous manipulation, the actions in these state-action pairs must impart the proper forces.

Dexterous manipulation demonstrations are most commonly collected via teleoperation, where robot actions are obtained by tracking human hand motion and retargeting this to robot positions [5]–[14]. Other works use retargeting to learn directly from human demonstrations [15, 16]. However, it remains challenging to use retargeting-based data

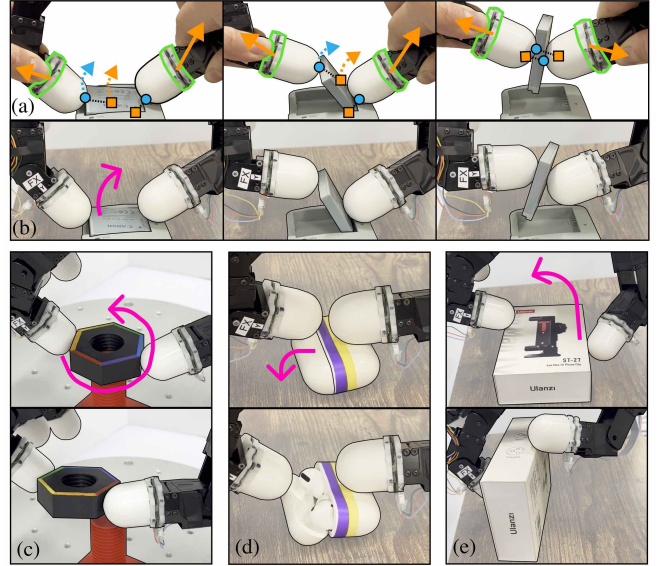


Fig. 1: (a) DexForce extracts force-informed actions (orange squares) from kinesthetic demonstrations by augmenting observed robot positions (blue circles) according to contact forces (orange arrows) measured with 6-axis force-torque sensors (green). (b) Executing force-informed actions allows the robot to reproduce forces applied in the kinesthetic demonstration, thereby executing the task. DexForce enables us to collect high-quality demonstrations for training policies on a variety of contact-rich tasks like (c) unscrewing a nut, (d) opening an AirPods case and (e) flipping a box.

collection methods to obtain demonstrations for tasks that require fine-grained dexterity. This is due to two inherent limitations. First, a human hand does not move like most robot hands; this kinematic difference, sometimes referred to as the “human-to-robot correspondence problem” [17, 18], makes it unintuitive for a human demonstrator to execute precise motions on a robot hand by moving their own hand [19]. Second, the demonstrator cannot feel what the robot feels during task execution; this lack of haptic feedback makes it especially difficult to execute actions that apply the correct forces to an object [20, 21].

Motivated by the shortcomings of current dexterous manipulation data collection methods, particularly for contact-rich tasks, we propose DexForce. The key element of DexForce is how actions are obtained. Given that successful contact-rich manipulation requires actions that apply the right forces, DexForce leverages contact forces, measured during kinesthetic demonstrations, to inform actions for policy learning. Kinesthetic teaching, where the demonstrator manually moves a robot to complete a task (Fig. 1a), provides a natural way of demonstrating contact-rich tasks; it not only allows the operator to utilize the full dexterity of the robot hand, but also gives the operator direct haptic feedback.

¹Stanford University, CA, USA.

Toyota Research Institute provided funds to support this work.

To record contact forces, we instrument the robot hand with 6-axis force-torque sensors mounted at the base of each fingertip (green in Fig. 1a). However, even when using a robot hand equipped with force sensing, kinesthetic demonstrations only provide state, namely the observed robot motion and measured forces; they do not provide the actions that would enable the robot to reproduce the measured forces. DexForce computes these actions, which we term *force-informed actions*, by augmenting observed robot motion according to the measured forces. When tracked with an impedance controller, these actions allow a robot to generate the right motion and forces to complete the task.

DexForce enables us to collect high-quality demonstrations for six contact-rich tasks, which we then use for imitation learning. Policies trained on our force-informed actions achieve an average success rate of 76% across all six tasks. In contrast, policies trained directly on actions that do not account for contact forces have near-zero success rates. This stark difference in performance underscores that our method of extracting force-informed actions is crucial for learning capable policies. We also study how including force data in policy observations impacts the performance of contact-rich manipulation policies. Our findings show that while including force in the observation improves policy performance for all six tasks, it matters most for tasks that require an advanced level of precision and coordination, like opening an AirPods case and unscrewing a nut.

In summary, we contribute:

- 1) DexForce, a method for collecting demonstrations of contact-rich dexterous manipulation tasks by using contact forces to extract force-informed actions from kinesthetic demonstrations, and
- 2) a study showing that including forces in policy observations results in larger policy performance improvements for tasks that demand greater precision and coordination.

II. RELATED WORK

Collecting dexterous hand demonstrations: This work proposes a solution for collecting demonstrations of fine-grained dexterous manipulation, which, as discussed in Section I, has been a limitation of widely-used retargeting-based data collection methods [5]–[16]. In particular, these methods lack haptic feedback and suffer from the human-to-robot correspondence problem. Other works also identify these shortcomings and use this observation to motivate their data collection methods [17, 22, 23].

Some works propose methods that mitigate the human-to-robot correspondence problem but still lack haptic feedback. ResPilot [22] improves retargeting-based teleoperation with residual Gaussian Process learning. However, it also relies on allowing the user to constrain robot fingertips to be a set distance away from the thumb, which makes it difficult to use their method for more general dexterity. Tilde [17] uses a twin robot to puppeteer a custom four-fingered hand. Puppeteering is a good way of circumventing the human-to-robot correspondence problem but has a high hardware

overhead. Critically, neither work provides the human operator with haptic feedback. The Tilde authors even note the lack of haptic feedback as a limitation of their system, stating that “tactile feedback could lead to more intentional and controlled interactions with objects in highly-dexterous tasks” [17]. DexForce leverages kinesthetic teaching, which not only avoids the human-to-robot correspondence problem, but also provides the user with direct haptic feedback.

In a similar family to kinesthetic teaching, “hand-over-hand” or “exoskeleton” methods are another promising paradigm for collecting demonstrations with robot hands. These methods make human hands move in a manner close to how robot hands move. Some works adapt exoskeletons for stroke rehabilitation [24, 25]. Another recent work introduces a wearable hand [23] for data collection, but does not equip the hand with force sensing. These works only demonstrate grasping motions, as opposed to the kinds of dexterous fingertip manipulation we consider.

Kinesthetic demonstrations with force sensing: Kinesthetic teaching is a well-established method for collecting demonstrations with robot arms [4]. It is typically used without force sensing for tasks that mostly require free-space motion. We focus our discussion on a smaller subset of works that have used kinesthetic teaching with force sensing with robot arms. Some works pair kinesthetic teaching with an additional haptic device to reproduce forceful interactions [26, 27]. More recent works use similar principles as DexForce to learn policies from kinesthetic demonstrations for robot arms [28, 29]. These works demonstrate their methods on tasks like opening and closing a door [29] or wiping a vase [28]. We further the findings of these works by showing that kinesthetic teaching with force sensing is also valuable for fine-grained dexterous manipulation.

Some prior works have used kinesthetic demonstrations to learn in-hand manipulation skills [30]–[32], but these works assume that the robot always maintains non-slipping contact with the object. Consequently, they are only capable of basic object re-orientation motions that can be done with a fixed grasp. [30] does use their method to demonstrate one task involving contact switching, but to achieve re-grasping, they need to supplement their method with additional hand-designed heuristics tailored to one object. In contrast, DexForce can be used for tasks with contact switching without the need for additional heuristics.

Open-loop strategies for in-hand manipulation: DexForce utilizes open-loop replay as part of its demonstration collection procedure. We are inspired by prior work that has shown the utility of open-loop strategies in complex dexterous manipulation. Like DexForce, [33] leverages open-loop replay to obtain real-world demonstrations. They replay rollouts of reinforcement learning (RL) policies that have been trained and rolled-out in simulation, whereas DexForce replays actions extracted from kinesthetic demonstrations. Their method hinges on first training successful RL policies in simulation, which requires extensive tuning for every new task. In contrast, kinesthetic teaching is easily applied to new tasks. They only show their method on the single task of spin-

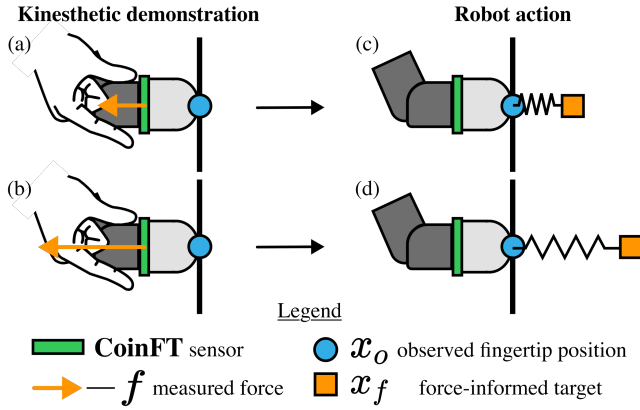


Fig. 2: The left column shows kinesthetic demonstrations where the operator applies (a) a small force and (b) a larger force to a surface. In both scenarios, even though the operator applies different amounts of force, the current fingertip position recorded during the demonstrations, denoted with a blue circle, is the same. The difference between the observed fingertip positions and force-informed targets is proportional to the contact force \mathbf{f} (c, d). Note: we visualize $-\mathbf{f}$, the contact force exerted by the object onto the finger.

ning cylindrical objects, whereas we demonstrate DexForce on six diverse tasks. [34] designs open-loop primitives for in-hand reorientation and finds that open-loop strategies can also lead to “surprisingly robust in-hand manipulation”.

Dexterous manipulation policies with force sensing: Many works, compiled in a recent survey [35], have studied how various types of tactile sensing affect policy learning. Our findings contribute to this body of work.

III. METHOD

DexForce obtains demonstrations of contact-rich dexterous manipulation by extracting force-informed actions from kinesthetic demonstrations on a robot hand. To measure contact forces, we equip the robot hand with 6-axis force-torque sensors at the base of each fingertip. As illustrated in Fig. 1a, with sensors at the base of each fingertip, the operator can firmly grip the robot finger anywhere above the sensor without impacting force measurements.

Kinesthetic demonstrations provide the robot state, consisting of observed fingertip positions $\mathbf{x}_o \in \mathbb{R}^3$ (blue circles in Fig. 2) and corresponding contact forces $\mathbf{f} \in \mathbb{R}^3$ (orange arrows), for each finger. For tasks that require the robot to apply forces to an object, the observed fingertip positions cannot be directly used as actions because they would not reproduce measured forces. Intuitively, this is because, as illustrated in Figs. 2a and 2b, no matter how much force the operator applies with the robot finger via kinesthetic teaching, the observed fingertip position remains the same.

To obtain the right actions for policy learning, we use the observed fingertip positions and measured forces to compute force-informed position targets. When used as input to a Cartesian impedance controller, these force-informed position targets enable the robot to generate the right motions and forces to complete the task.

In the following sections, we will first describe the impedance controller. Then, we will present our method for extracting force-informed actions from kinesthetic demonstration data. Finally, we will present the complete two-stage

DexForce demonstration collection procedure and how we use these demonstrations to learn policies.

Cartesian impedance control: Impedance control [36] models the relationship between force and motion as a second-order mechanical system, characterized by a given mass, damping, and stiffness [37]. It provides a means of producing desired motion and forces, instead of using explicit force control to directly track forces. Force control is notoriously unstable, especially when tasks involve discontinuous contact with the environment [38].

In a Cartesian impedance controller, the control force $\mathbf{F} \in \mathbb{R}^3$ for one finger is given as

$$\mathbf{F} = \mathbf{K}_p(\mathbf{x}_d - \mathbf{x}_c) - \mathbf{K}_v(\dot{\mathbf{x}}_c) \quad (1)$$

where the first term scales the error between the desired and current fingertip positions \mathbf{x}_d and \mathbf{x}_c , respectively, by a stiffness gain matrix \mathbf{K}_p , and the second term adds damping by scaling the fingertip velocity $\dot{\mathbf{x}}_c$ by the gain matrix \mathbf{K}_v . We use diagonal matrices with a constant value on the diagonal for both \mathbf{K}_p and \mathbf{K}_v . We tune the controller gains such that the fingertips follow a desired position trajectory while moving in free space. To apply this control force, we command the finger with joint torques $\boldsymbol{\tau}$, given as

$$\boldsymbol{\tau} = \mathbf{J}^T \mathbf{F} + \mathbf{g} \quad (2)$$

where \mathbf{J} is the finger Jacobian and \mathbf{g} is a gravity compensation term.

Computing force-informed position targets: Using impedance control enables a robot to apply forces by tracking desired positions. Given an observed fingertip position \mathbf{x}_o and measured contact force \mathbf{f} from a kinesthetic demonstration, our goal is to compute a desired fingertip position that produces \mathbf{f} when tracked with the controller in Eq. (2). We term this desired position a *force-informed target*, \mathbf{x}_f .

The first term of the control law in Eq. (1) models the relationship between force and displacement as a spring. Assuming quasi-static motion, it follows that we can use the same model to compute a force-informed target \mathbf{x}_f as a function of an observed fingertip position \mathbf{x}_o and the contact force \mathbf{f} exerted by the finger onto the object,

$$\mathbf{x}_f = \mathbf{x}_o + \mathbf{K}_f \mathbf{f} \quad (3)$$

where \mathbf{K}_f is a hand-tuned stiffness matrix. Intuitively, when an operator presses the robot fingertip onto a surface during a kinesthetic demonstration (Figs. 2a and 2b), the force-informed target will move farther into the surface as the applied force increases (Figs. 2c and 2d). While Eq. (3) does not model soft contact or friction, we empirically find it to be a sufficient model for many tasks.

DexForce demonstration collection procedure The DexForce demonstration collection procedure consists of two stages. Fig. 3 depicts this two-stage procedure on an example task where one finger must slide a square along a fixed rail into the red goal region.

In **Stage 1**, we extract force-informed targets from a kinesthetic demonstration. From a kinesthetic demonstration, we record the robot state, consisting of a T timestep-long trajectory of observed fingertip positions $\mathbf{x}_{o,1} \dots \mathbf{x}_{o,T}$ (blue circles in Fig. 3) and corresponding contact forces $\mathbf{f}_1 \dots \mathbf{f}_T$ (orange arrows), for each finger. With this data, we compute

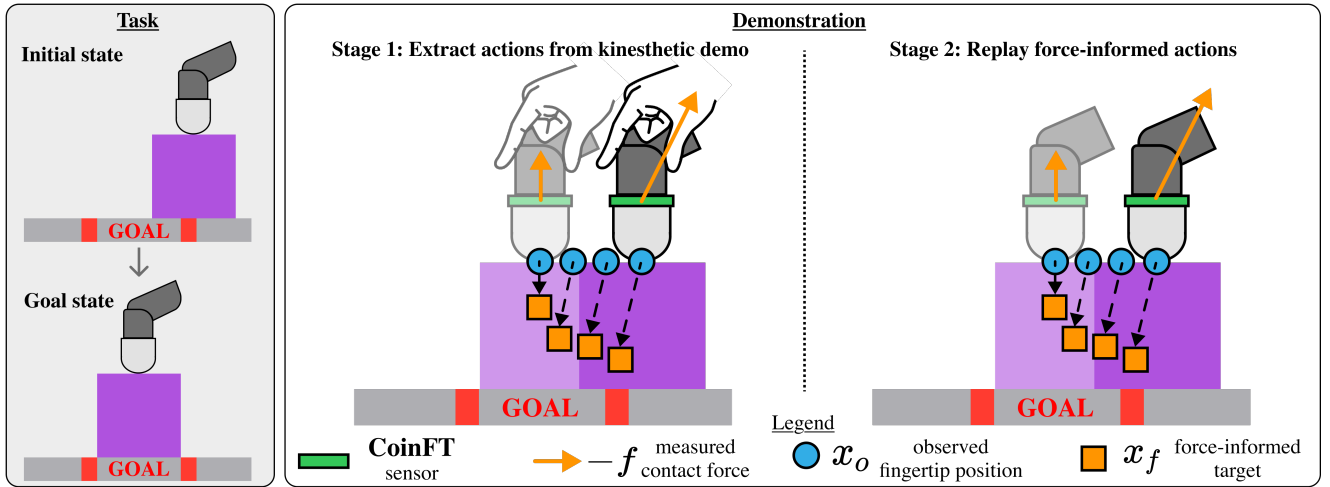


Fig. 3: The DexForce two-stage demonstration collection procedure, illustrated with a one-finger task where the robot must slide a purple square along a fixed surface to the red goal region. Note: we visualize $-f$, the contact force exerted by the object onto the finger.

a trajectory of force-informed position targets $\mathbf{x}_{f,1} \dots \mathbf{x}_{f,T}$ (orange squares) using Eq. (3).

In **Stage 2**, we obtain the final demonstration used for policy learning. These demonstrations should also include images to give policies a visual understanding of the scene. However, images of a kinesthetic demonstration would contain the operator’s hand, whereas test-time images only contain the robot. As such, the kinesthetic demonstrations collected in Stage 1 cannot be used directly to train policies. To obtain robot-only demonstrations that match test-time conditions, we replay the kinesthetic demonstration by tracking the trajectory of force-informed targets $\mathbf{x}_{f,1} \dots \mathbf{x}_{f,T}$, computed in Stage 1, with the Cartesian impedance controller in Eq. (2). We tune the spring stiffness \mathbf{K}_f in Eq. (3) such that these replays successfully re-produce kinesthetic demonstrations. We use $\mathbf{K}_f = (1/220) * \mathbf{I}_3$, where \mathbf{I}_3 is the 3×3 identity matrix, for all tasks. Additionally, we use a wrist-mounted camera to capture image observations. From this replay, we record the new observed fingertip positions $\mathbf{x}_{o,1}^* \dots \mathbf{x}_{o,T}^*$, contact forces $\mathbf{f}_1^* \dots \mathbf{f}_T^*$, contact moments $\mathbf{m}_1^* \dots \mathbf{m}_T^*$, and images $\mathbf{I}_1 \dots \mathbf{I}_T$.

Policy learning: We use DexForce demonstrations to train Diffusion Policies [3]. An observation at timestep t consists of image features of image \mathbf{I}_t concatenated with the Stage 2 contact forces \mathbf{f}_t^* and moments \mathbf{m}_t^* of each finger. The policy outputs force-informed targets, which we execute with the impedance controller in Eq. (2). We supervise policy training on force-informed targets \mathbf{x}_f .

IV. EXPERIMENTS

We conduct experiments to answer the following three questions:

- 1) How important is using DexForce’s force-informed actions to the success of imitation learning?
- 2) How does including contact forces in policy observations impact policy performance?
- 3) How well do policies generalize to out-of-distribution scenarios with different force characteristics?

Tasks: We evaluate policies on six contact rich manipulation tasks: `slide cube`, `reorient smiley`,

`open AirPods`, `grasp battery`, `unscrew nut`, and `flip box`. Fig. 4 provides a description, an example trajectory, success criteria, and the number of training demonstrations used to train each task policy. We choose a variety of tasks that require different contact-rich interactions, like applying precise forces and making and breaking contact with the object. Because a human operator can comfortably collect kinesthetic demonstrations with up to two robot fingers, we design tasks to use one or two fingers. In future work, we will explore mechanisms that enable an operator to collect kinesthetic demonstrations with more robot fingers.

In our evaluation, we label policy rollouts with one of three outcomes: success, failure, or partial success. Partial successes are scenarios where the robot makes progress towards completing the task but fails to apply the right forces to fully complete the task. For example, for `reorient smiley`, a partial success is when the robot has flipped the block at least once but failed to flip it to the correct orientation. We refer the reader to Fig. 4 for the partial success criteria of each task. Recording partial successes helps us understand failure modes of policies.

For each task, we vary the initial configuration of the object in both training demonstrations and evaluation scenes. As shown in Fig. 5, for `slide cube`, `reorient smiley`, `open AirPods`, `grasp battery`, and `flip box`, we vary the object pose within the reachable workspace of the Allegro hand. For `unscrew nut`, we vary how much the nut is screwed onto its mount. To ensure consistency across all policy evaluations, within each task, we evaluate all policies on the same 30 random initial object configurations.

Hardware setup: We conduct our experiments on an Allegro Hand instrumented with a wrist-mounted camera and 6-axis force-torque sensors at the bases of the thumb and index fingers, as shown in Fig. 6. To capture RGB images, we use a wrist-mounted RealSense D435 camera fitted with a fisheye lens. As shown in Fig. 6, the fisheye lens is necessary to capture the entire workspace of the hand. For the force-torque sensors, we use CoinFT [39] sensors.

Task name description	Example task trajectory			Success criteria			# demos
	initial	→	final	Success	Partial success	Failure	
slide cube slide cube along fixed rail to red goal region with one finger		→					80
reorient smiley re-orient smiley-face block with one finger		→					60
open AirPods open AirPods case with two fingers		→					150
grasp battery grasp camera battery with two fingers		→					110
unscrew nut unscrew and lift nut with two fingers		→					80
flip box flip box onto its side with two fingers		→					70

Fig. 4: Task names, descriptions, example trajectories, success criteria, and number of training demonstrations.

Policy learning details: We train CNN-based Diffusion Policies [3] for all tasks. We use ResNet18 to encode RGB images. We use an observation horizon of 2, an action prediction horizon of 16, and an action execution horizon of 8. We train policies for 1000 epochs. We record demonstrations at 30Hz and downsample to 10Hz for training. For `slide cube`, `reorient smiley`, `open AirPods`, `unscrew nut`, and `flip box`, we use an image size of [128, 128] pixels. To better capture image details for `grasp battery`, we use an image size of [256, 256] pixels.

Question 1) How important is using force-informed actions to the success of imitation learning? For each task, we compare a policy trained on our force-informed targets to a policy trained directly on the observed fingertip positions, which do not account for contact forces. For policies trained on the observed fingertip positions, we use the next timestep’s observed fingertip position as the action. All policies are trained with observations that consist of the RGB image features concatenated with the contact forces and moments for each finger.

As shown in Fig. 7, policies trained on our force-informed targets achieve success rates ranging from 90% on the `slide cube` task to 57% on the `open AirPods` task. Across all six tasks, the force-informed action policies achieve an average success rate of 76%. In contrast, policies trained directly on observed fingertip positions have near-zero success rates on all six tasks. This stark difference in performance demonstrates the importance of computing inferences based on measured contact forces.

Policies trained on observed fingertip positions fail because commanding the fingertips to go to those positions does not generate the right forces to complete tasks. For most tasks, the robot is able to move its fingers to the object but fails to apply any force, resulting in failures. On `unscrew nut`, the policy trained on observed fingertip positions achieves partial success on 23 out of 30 trials, where it is able to unscrew the nut. Yet, it never grasps the nut to fully complete the task. This suggests that force-informed actions are most important for the grasping part of the task. In policy rollouts, we observe that the hexagonal shape of

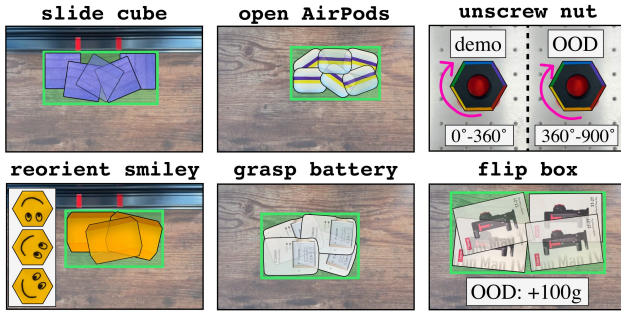


Fig. 5: In our demonstrations, we randomly initialize object poses within the green regions. For our in-distribution evaluations, we sample 30 initial poses from within these green regions. For the unscrew nut demonstrations, we fix the position of the mount and randomize the initial rotation of the nut between 0° - 360° . OOD scenarios: For unscrew nut, initial rotation of nut between 360° - 900° . For flip box, place 100g weight inside box.

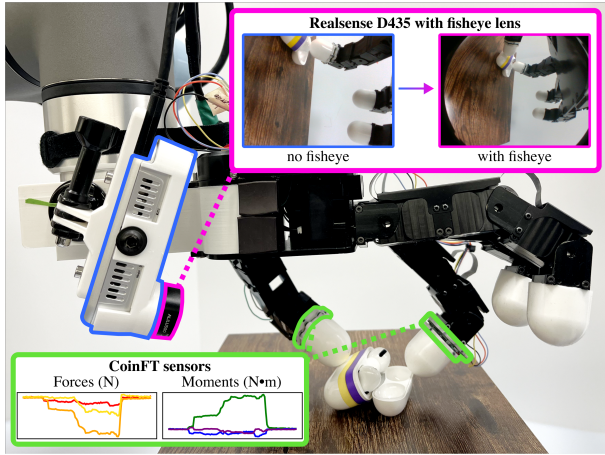


Fig. 6: Hardware setup: Allegro hand, wrist-mounted RealSense D435 camera (blue), to capture RGB images, with a fisheye lens attachment (pink), which increases the camera field of view to capture the entire workspace of the hand, and two CoinFT sensors [39] (green) mounted at the bases of the thumb and index finger, to record 6-axis force-torque measurements.

the nut allows the robot to unscrew the nut by pushing on the corners instead of squeezing the nut to twist it. We refer the reader to our supplementary video for examples.

While the force-informed policy has the lowest success rate on open AirPods, achieving a full success on this task by opening the case completely is quite difficult. If the robot just partially opens the lid, the case will close itself under its own weight. For the case to remain open, the robot must apply the right forces to fully open the lid. We consider partially opening the case to be a partial success, because the robot still applies some meaningful force to the object. The force-informed policy achieves success on 17/30 trials and partial success on another 8 trials.

Question 2: How does including contact forces in observations impact policy performance? In the prior section, we show that training on force-informed actions is critical for policy learning. Next, we ablate the inclusion of force data in policy observations to study how force observations impact policy performance. We supervise all policies on DexForce’s force-informed targets. For all tasks, we train three policies with the following observation ablations:

- **RGB, F/T**: RGB image features concatenated with the raw

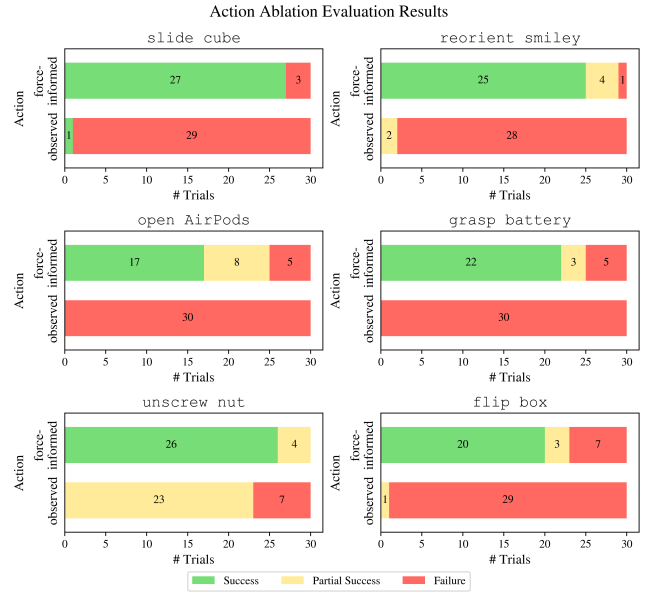


Fig. 7: Using force-informed actions to train policies is critical for policy learning success. Policies trained directly on observed fingertip positions, which do not account for contact forces, have near-zero success rates.

6-axis contact force and moment vectors for each finger.

- **RGB, 0/1**: RGB image features concatenated with a binary contact signal for each finger. The contact signal is 1 if the finger is in contact (magnitude of the measured force exceeds 0.55N), and 0 if the finger is not in contact. We include this ablation because other work [40] has shown that binary contact information is sufficient for dexterous manipulation.

- **RGB only**: RGB image features only. No force information.

Fig. 8 shows the results of this study. We find that while including 6-dimensional force data in policy observations improves success rates for all tasks, it benefits open AirPods, unscrew nut, and slide cube the most. For these three tasks, **RGB, F/T** policies have statistically significant success rate increases over **RGB-only** policies, improving performance on open AirPods by 1600%, unscrew nut by 136%, and slide cube by 58.8%.

Out of the six tasks, these three tasks demand the most precision and coordination. **RGB-only** policies fail more often than **RGB, F/T** policies because the robot fails to apply forces that meet the required level of precision and coordination. For open AirPods, the **RGB-only** policy often pushes down on the lid of the case too hard and in the wrong direction, thus failing to move the lid at all. For unscrew nut, the **RGB-only** policy either fails to unscrew or grasp the nut. For slide cube, the **RGB-only** policy does not apply the right forces to slide the cube to the goal. We refer the reader to our supplementary video for examples.

We find that using binary contact information in policy observations is not comparable to using 6-axis contact force data; across all six tasks, **RGB, 0/1** policies have lower success rates than **RGB, F/T** policies. Furthermore, **RGB, 0/1** policies tend to do equivalently, or worse, than **RGB-only** policies, as shown in Fig. 8. This suggests that binary

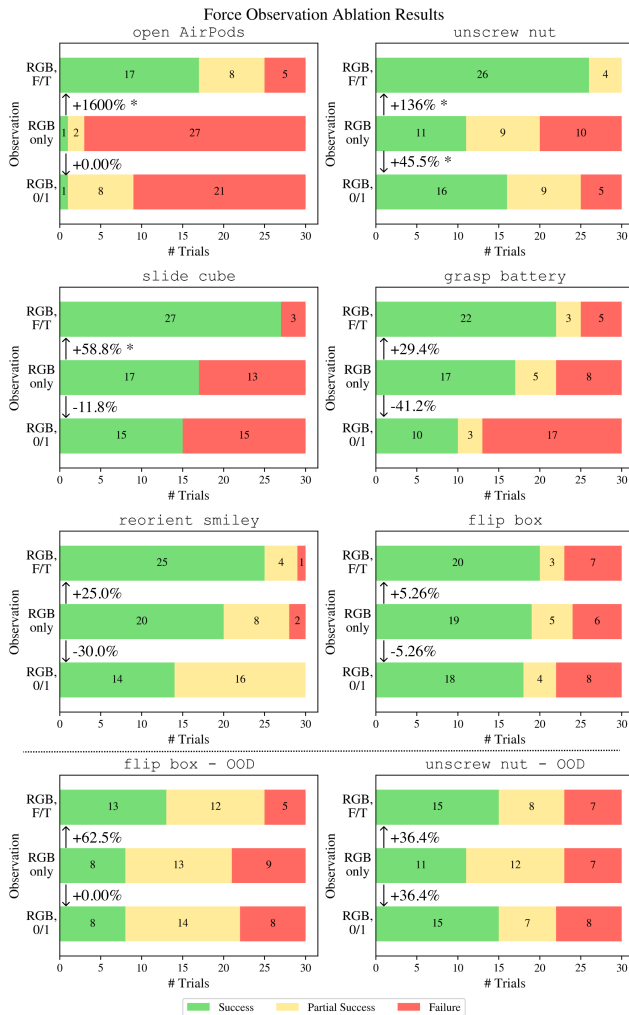


Fig. 8: Force observation ablation results for six in-distribution evaluations (first three rows) and two out-of-distribution (OOD) evaluations (bottom row). In each plot, we show the success rate increase or decrease from **RGB-only** policies to **RGB, F/T** and **RGB, 0/1** policies (arrows between bars). * denotes statistical significance (two-proportion z-test, $\alpha = 0.05$). For the in-distribution evaluations, plots are ordered from highest to lowest success rate increase from **RGB-only** to **RGB, F/T**. The *open AirPods*, *unscrew nut*, and *slide cube* tasks benefit the most from force observations.

finger tip contact signals do not provide useful contact information to solve contact-rich tasks.

We also ablate the inclusion of proprioception on a smaller subset of tasks. We find, as shown in Fig. 9, that policies with proprioception tend to perform worse than policies without it. [41] obtains similar findings and attributes this to causal confusion between the proprioceptive information and actions [42]. As such, in our force observation ablation study, we chose to omit proprioception from observations. Even on policies trained with proprioception, we see that policies with force do better than those without force, which matches the trend in policies trained without proprioception.

Question 3: How well do policies generalize to out-of-distribution scenarios with different force characteristics?

Finally, we test policies on out-of-distribution (OOD) task variations. We design OOD scenarios that look similar to the demonstrations but have different force characteristics.

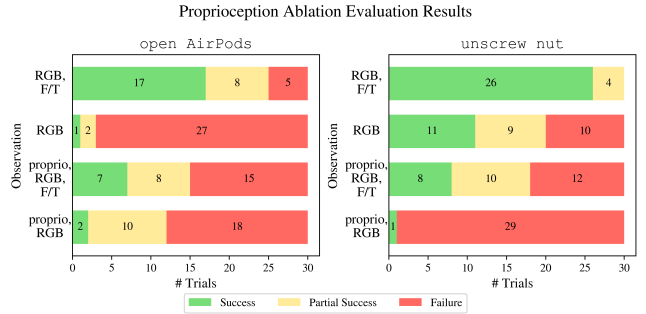


Fig. 9: Proprioception ablation results. Policies with proprioception (bottom two bars in each plot) tend to perform worse than policies without it.

In *unscrew nut* demonstrations, we vary the amount nut is screwed onto the mount between 0-1 revolution (0° - 360°). In our *unscrew nut* - OOD evaluation, we initialize the nut rotation to be between 1-2.5 revolutions (360° - 900°). In *flip box* - OOD, we place a 100g weight inside the box.

As expected, for both tasks, policies perform worse on OOD scenarios (last row of Fig. 8) than on their in-distribution counterparts. For *flip box* - OOD, the increased mass makes the robot more susceptible to only partially flipping the box, raising the number of partial successes of **RGB, F/T** policies from 3, in the in-distribution case, to 12, in the OOD case. Still, policies are able to successfully complete tasks about 50% of the time, despite not being trained on these more challenging task variants. In *unscrew nut* - OOD, the robot can still pick up the nut, despite having to rotate the nut much more. Furthermore, policies in the observation perform better than policies that do not see force data.

V. CONCLUSION

We present DexForce, a method for collecting demonstrations of dexterous manipulation tasks by using measured forces to extract force-informed actions from kinesthetic demonstrations. DexForce enables us to demonstrate contact-rich tasks that are difficult to demonstrate using current widely-used retargeting-based data collection methods. Policies trained on our force-informed actions achieve an average success rate of 76% across six tasks, whereas policies trained on actions that do not account for contact forces have near-zero success rates.

While we acknowledge that DexForce may not be best suited for large-scale data collection, it shows how we can obtain actions that account for contact forces and that these force-informed actions are valuable for policy learning. We hope that these insights not only enhance existing data collection methods [23, 43], but also inform the design of future methods. Additionally, DexForce is a valuable research tool that makes it possible for us to study the impact of force-sensing on imitation learning for contact-rich dexterous manipulation. In future work, we will study alternative means of providing demonstrations that retain the benefits of kinesthetic teaching, namely methods that allow the operator to use full dexterity of robot and provide direct haptic feedback.

REFERENCES

- [1] T. Z. Zhao, V. Kumar, S. Levine, and C. Finn, "Learning Fine-Grained Bimanual Manipulation with Low-Cost Hardware," in *Proceedings of Robotics: Science and Systems*, Daegu, Republic of Korea, July 2023.
- [2] T. Z. Zhao, J. Tompson, D. Driess, P. Florence, K. Ghasemipour, C. Finn, and A. Wahid, "Aloha unleashed: A simple recipe for robot dexterity," 2024. [Online]. Available: <https://arxiv.org/abs/2410.13126>
- [3] C. Chi, S. Feng, Y. Du, Z. Xu, E. Cousineau, B. Burchfiel, and S. Song, "Diffusion policy: Visuomotor policy learning via action diffusion," in *Proceedings of Robotics: Science and Systems (RSS)*, 2023.
- [4] H. Ravichandar, A. S. Polydoros, S. Chernova, and A. Billard, "Recent advances in robot learning from demonstration," *Annual Review of Control, Robotics, and Autonomous Systems*, vol. 3, no. Volume 3, 2020, pp. 297–330, 2020. [Online]. Available: <https://www.annualreviews.org/content/journals/10.1146/annurev-control-100819-063206>
- [5] S. P. Arunachalam, I. Güzey, S. Chintala, and L. Pinto, "Holo-dex: Teaching dexterity with immersive mixed reality," 2022. [Online]. Available: <https://arxiv.org/abs/2210.06463>
- [6] X. Cheng, J. Li, S. Yang, G. Yang, and X. Wang, "Open-television: Teleoperation with immersive active visual feedback," *arXiv preprint arXiv:2407.01512*, 2024.
- [7] A. Handa, K. V. Wyk, W. Yang, J. Liang, Y.-W. Chao, Q. Wan, S. Birchfield, N. Ratliff, and D. Fox, "Dexpilot: Vision based teleoperation of dexterous robotic hand-arm system," 2019. [Online]. Available: <https://arxiv.org/abs/1910.03135>
- [8] A. Iyer, Z. Peng, Y. Dai, I. Guzey, S. Haldar, S. Chintala, and L. Pinto, "Open teach: A versatile teleoperation system for robotic manipulation," 2024.
- [9] Y. Qin, W. Yang, B. Huang, K. Van Wyk, H. Su, X. Wang, Y.-W. Chao, and D. Fox, "Anytelego: A general vision-based dexterous robot arm-hand teleoperation system," in *Robotics: Science and Systems*, 2023.
- [10] B. Romero, H.-S. Fang, P. Agrawal, and E. Adelson, "Eyesight hand: Design of a fully-actuated dexterous robot hand with integrated vision-based tactile sensors and compliant actuation," 2024. [Online]. Available: <https://arxiv.org/abs/2408.06265>
- [11] K. Shaw, Y. Li, J. Yang, M. K. Srirama, R. Liu, H. Xiong, R. Mendonca, and D. Pathak, "Bimanual dexterity for complex tasks," in *8th Annual Conference on Robot Learning*, 2024.
- [12] S. Yang, M. Liu, Y. Qin, D. Runyu, L. Jialong, X. Cheng, R. Yang, S. Yi, and X. Wang, "Ace: A cross-platform visual-exoskeletons for low-cost dexterous teleoperation," *arXiv preprint arXiv:2407.01512*, 2024.
- [13] R. Ding, Y. Qin, J. Zhu, C. Jia, S. Yang, R. Yang, X. Qi, and X. Wang, "Bunny-visionpro: Real-time bimanual dexterous teleoperation for imitation learning," 2024. [Online]. Available: <https://arxiv.org/abs/2407.03162>
- [14] P. Mannam, K. Shaw, D. Bauer, J. Oh, D. Pathak, and N. Pollard, "Designing anthropomorphic soft hands through interaction," 2024. [Online]. Available: <https://arxiv.org/abs/2306.04784>
- [15] C. Wang, H. Shi, W. Wang, R. Zhang, L. Fei-Fei, and C. K. Liu, "Dexcap: Scalable and portable mocap data collection system for dexterous manipulation," *arXiv preprint arXiv:2403.07788*, 2024.
- [16] S. Chen, C. Wang, K. Nguyen, L. Fei-Fei, and C. K. Liu, "Arcap: Collecting high-quality human demonstrations for robot learning with augmented reality feedback," *arXiv preprint arXiv:2410.08464*, 2024.
- [17] Z. Si, K. L. Zhang, Z. Temel, and O. Kroemer, "Tilde: Teleoperation for dexterous in-hand manipulation learning with a deltax hand," *arXiv preprint arXiv:2405.18804*, 2024.
- [18] M. Arduengo, A. Arduengo, A. Colome, J. Lobo-Prat, and C. Torras, "Human to robot whole-body motion transfer," in *2020 IEEE-RAS 20th International Conference on Humanoid Robots (Humanoids)*. IEEE, Jul. 2021, p. 299–305. [Online]. Available: <http://dx.doi.org/10.1109/HUMANOIDS47582.2021.9555769>
- [19] P. Wu, Y. Shentu, Z. Yi, X. Lin, and P. Abbeel, "Gello: A general, low-cost, and intuitive teleoperation framework for robot manipulators," 2023.
- [20] D. Morris, H. Tan, F. Barbagli, T. Chang, and K. Salisbury, "Haptic feedback enhances force skill learning," in *Second Joint EuroHaptics Conference and Symposium on Haptic Interfaces for Virtual Environment and Teleoperator Systems (WHC'07)*, 2007, pp. 21–26.
- [21] P. Ström, L. Hedman, L. Särnå, A. Kjellin, T. Wredmark, and L. Felländer-Tsai, "Early exposure to haptic feedback enhances performance in surgical simulator training: A prospective randomized crossover study in surgical residents," *Surgical endoscopy*, vol. 20, pp. 1383–8, 10 2006.
- [22] P. Naughton, J. Cui, K. Patel, and S. Iba, "Respilot: Teleoperated finger gaiting via gaussian process residual learning," in *Conference on Robot Learning (CoRL)*, 2024.
- [23] D. Wei and H. Xu, "A wearable robotic hand for hand-over-hand imitation learning," in *2024 IEEE International Conference on Robotics and Automation (ICRA)*, 2024, pp. 18 113–18 119.
- [24] H. Dai, Z. Lu, M. He, and C. Yang, "A gripper-like exoskeleton design for robot grasping demonstration," in *Actuators*, vol. 12, no. 1. MDPI, 2023, p. 39.
- [25] Z. Lu, L. Chen, H. Dai, H. Li, Z. Zhao, B. Zheng, N. F. Lepora, and C. Yang, "Visual-tactile robot grasping based on human skill learning from demonstrations using a wearable parallel hand exoskeleton," *IEEE Robotics and Automation Letters*, 2023.
- [26] K. Kronander and A. Billard, "Learning compliant manipulation through kinesthetic and tactile human-robot interaction," *IEEE Transactions on Haptics*, vol. 7, no. 3, pp. 367–380, 2014.
- [27] S. C. Petar Kormushev and D. G. Caldwell, "Imitation learning of positional and force skills demonstrated via kinesthetic teaching and haptic input," *Advanced Robotics*, vol. 25, no. 5, pp. 581–603, 2011. [Online]. Available: <https://doi.org/10.1163/016918611X558261>
- [28] Y. Hou, Z. Liu, C. Chi, E. Cousineau, N. Kuppaswamy, S. Feng, B. Burchfiel, and S. Song, "Adaptive compliance policy: Learning approximate compliance for diffusion guided control," 2024. [Online]. Available: <https://arxiv.org/abs/2410.09309>
- [29] T. Ablett, O. Limoyo, A. Sigal, A. Jilani, J. Kelly, K. Siddiqi, F. Hogan, and G. Dudek, "Multimodal and force-matched imitation learning with a see-through visuotactile sensor," 2024. [Online]. Available: <https://arxiv.org/abs/2311.01248>
- [30] M. Li, H. Yin, K. Tahara, and A. Billard, "Learning object-level impedance control for robust grasping and dexterous manipulation," in *2014 IEEE International Conference on Robotics and Automation (ICRA)*, 2014, pp. 6784–6791.
- [31] G. Solak and L. Jamone, "Learning by demonstration and robust control of dexterous in-hand robotic manipulation skills," in *2019 IEEE/RSJ International Conference on Intelligent Robots and Systems (IROS)*, 2019, pp. 8246–8251.
- [32] —, "Haptic exploration of unknown objects for robust in-hand manipulation," *IEEE Transactions on Haptics*, vol. 16, no. 3, pp. 400–411, 2023.
- [33] J. Wang, Y. Yuan, H. Che, H. Qi, Y. Ma, J. Malik, and X. Wang, "Lessons from learning to spin 'pens'," in *CoRL*, 2024.
- [34] A. Bhatt, A. Sieler, S. Puhlmann, and O. Brock, "Surprisingly Robust In-Hand Manipulation: An Empirical Study," in *Proceedings of Robotics: Science and Systems*, Virtual, July 2021.
- [35] A. I. Weinberg, A. Shirizly, O. Azulay, and A. Sintov, "Survey of learning-based approaches for robotic in-hand manipulation," 2024. [Online]. Available: <https://arxiv.org/abs/2401.07915>
- [36] N. Hogan, "Impedance control: An approach to manipulation," in *1984 American Control Conference*, 1984, pp. 304–313.
- [37] B. Siciliano and O. Khatib, Eds., *Springer Handbook of Robotics*. Berlin, Heidelberg: Springer, 2008. [Online]. Available: <http://dx.doi.org/10.1007/978-3-540-30301-5>
- [38] R. Balachandran, M. Jorda, J. Artigas, J.-H. Ryu, and O. Khatib, "Passivity-based stability in explicit force control of robots," in *2017 IEEE International Conference on Robotics and Automation (ICRA)*, 2017, pp. 386–393.
- [39] K. T. Yoshida, Z. A. Zook, H. Choi, M. Luo, M. K. O'Malley, and A. M. Okamura, "Design and evaluation of a 3-dof haptic device for directional shear cues on the forearm," *IEEE Transactions on Haptics*, vol. 17, no. 3, pp. 483–495, 2024.
- [40] Z.-H. Yin, B. Huang, Y. Qin, Q. Chen, and X. Wang, "Rotating without seeing: Towards in-hand dexterity through touch," *Robotics: Science and Systems*, 2023.
- [41] Octo Model Team, D. Ghosh, H. Walke, K. Pertsch, K. Black, O. Mees, S. Dasari, J. Hejna, C. Xu, J. Luo, T. Kreiman, Y. Tan, L. Y. Chen, P. Sanketi, Q. Vuong, T. Xiao, D. Sadigh, C. Finn, and S. Levine, "Octo: An open-source generalist robot policy," in *Proceedings of Robotics: Science and Systems*, Delft, Netherlands, 2024.
- [42] P. de Haan, D. Jayaraman, and S. Levine, "Causal confusion in imitation learning," 2019. [Online]. Available: <https://arxiv.org/abs/1905.11979>
- [43] C. Chi, Z. Xu, C. Pan, E. Cousineau, B. Burchfiel, S. Feng, R. Tedrake, and S. Song, "Universal manipulation interface: In-the-wild robot teaching without in-the-wild robots," in *Proceedings of Robotics: Science and Systems (RSS)*, 2024.